# Multiparameter microwave retrieval algorithms: performance of neural networks

**R. M. Gairola*, Samir Pokhrel, A. K. Varma and Vijay K. Agarwal**

Oceanic Sciences Division, Meteorology and Oceanography Group, Space Applications Centre, Ahmedabad 380 015, India

**The present study deals with a major aspect of retrieval of oceanic and atmospheric parameters from Tropical Rainfall Measuring Mission-Microwave Imager (TRMM-TMI) channels following the sensitivity studies carried out earlier based on radiative transfer model simulations for rain-free atmospheric conditions over the global tropical oceans. The potentiality of artificial neural network (ANN) for retrieval of geophysical parameters like wind speed, total precipitable water (TPW) and cloud liquid water (CLW) from TMI has been investigated. The radiative transfer simulations of brightness temperatures (TBs) performed for TRMM-TMI frequencies with the inputs from the European Centre for Medium Range Weather Forecast (ECMWF) fields of geophysical parameters were used for the constitution of the database of input and output field vectors for the ANN applications. The results show that the neural network algorithm has the capacity to perform retrieval of ocean–atmospheric parameters with good accuracy.**

**Keywords:** Algorithm, microwave, neural network.

DURING the past several years, the use of satellite-based microwave radiometers for continuous observations of ocean and atmosphere has become common practice. The use of well-calibrated satellite-based microwave radiometers makes it possible to obtain long time series of geophysical parameters. Over the oceans, these parameters include three phases of water: total precipitable water (TPW), cloud liquid water (CLW) and rainfall as well as surface parameters like the sea surface wind speed (WS) and sea surface temperature (SST). The parameters are highly useful in a wide variety of studies of hydrological processes[1] and can improve weather prediction via data assimilation into operational models[2,3]. In order for the satellites to provide the best possible performance in providing most accurate geophysical parameters, it is pertinent to explore the newly emerging techniques in the field of retrievals. The major objective of this paper was to develop a retrieval algorithm for non-raining oceanic and atmospheric parameters like the WS, TPW, and CLW for the Tropical Rainfall Measuring Mission-Microwave Imager (TRMM-TMI) radiometric channels to a desired accuracy based on artificial neural network (ANN) approach as a prelude to the MADRAS (Microwave Analysis and Detection of Rain and Atmospheric Systems) sensor of Megha-Tropiques mission under Indo-French joint programme which will have almost similar frequencies as those of TRMM-TMI.

Recently ANN has been recognized as being useful for retrieval operations in remote sensing of the ocean and atmosphere. The use of ANN in statistical estimation is often effective because it can simultaneously address nonlinear dependencies and complex statistical behaviour. It has been shown that a multilayer perceptron[4] with a single hidden layer and nonlinear activation function is capable of approximating any real valued continuous function, provided a sufficient number of units within the hidden layer exists[5]. Several studies have been conducted earlier, for retrieval of sea surface wind[6,7], total precipitable water[8–10] and integrated cloud liquid water[11–14] parameters using mainly Special Sensor Microwave Imager (SSM/I) data and multiple regression approach. More recently, a methodology for the formulation of multiparameter and multi-instrument retrieval from TRMM was developed by Obligis *et al.*[15]. The performance of ANN approach compared to the multiple regression approach has recently been made[16], for retrieval of TPW and CLW with the SSM/I observations. The present attempt is to evaluate the performance of ANN approach for retrieval of all the above-mentioned parameters using simulated database from radiative transfer model for TRMM-TMI radiometric channels. The ANN approach used here is based on a multilayer perceptron developed by Moreau *et al.*[17].

The main input database for radiative transfer simulations is from a set of ECMWF forecast fields, representing tropical regions of the globe mainly during monsoon period over the Indian Ocean and Indian sub-continent. About 25,368 atmospheric profiles were used for the simulations through a radiative transfer model from Prigent *et al.*[18] that constitutes the vertical profiles of temperature, pressure, specific humidity and CLW defined on 31 vertical levels and the pressure, temperature and specific humidity at the surface and wind speed at 10 m height. The horizontal resolution of these data are $1.125° \times 1.125°$ in latitude and longitude, which corresponds to a 125 km horizontal mesh at the equator. The model simulated brightness temperatures (TBs) and the corresponding ECMWF forecast fields of the main geophysical parameters of interest are used here as the input and output field vectors for designing the ANN architecture both for training and testing purposes.

Given accurate and reliable input and output field vectors, geophysical retrieval algorithms can be developed using various approaches. As stated earlier, we have used the ANN approach, on the database using the radiative transfer simulations for TMI channels (10, 18.7, 21, 37 and 85 GHz) for both horizontal (H) and vertical (V) polarization except for a single-V polarization at 21 GHz, with the ECMWF fields of oceanic and atmospheric variables.

*For correspondence. (e-mail: rmgairola@yahoo.com)

A brief description of ANN, relevant for this paper is given below.

An ANN may be viewed as a mathematical model composed of many nonlinear computational elements, named neurons, operating in parallel and massively connected by links characterized by different weights. A single neuron computes the sum of its inputs, adds a bias term, and drives the result through a generally nonlinear activation function to produce a single output termed 'the activation level of the neuron'. ANN models are mainly specified by the network topology, neuron characteristics, and training or learning rules[19]. The term 'topology' refers to the architecture of the network as a whole: the number of its input, output and hidden units and their interconnection. For this study, a three layer feed-forward neural network is used. It consists mainly of three layers of fully connected nodes. As stated earlier, each hidden or output node in the network receives a 'signal' from each node in a previous layer; these signals are summed and are fed in an activation function to produce a single output signal for that node (Figure 1). The sigmoid function was chosen as the activation function for all the nodes in the hidden layer, given by

$$f(x) = 1/(1 + e^{-x}).$$

The sigmoid activation function squashes the input which may have values between plus and minus infinity, to yield these values in the range [0, 1]. The multilayer perceptron is designed to approximate an unknown input–output relation by determining the weight and strength of each connection via learning rules. These rules indicate how to pursue minimization of the error function measuring the quality of the network's approximation on the restricted domain covered by a training set. In the present case the error minimization is done using the back propagation algorithm[20]. Output for the first hidden node, say $y_1$ is given by

$$y_1 = f\left(\sum_{i=1}^{n} w_{1i}x_i + \phi\right)$$

and similarly for $y_2$ and output nodes and so on. Here $f$ is the activation function given above, $w_{1i}$ is the weight connecting $y_1$ to $i$th input and $\phi$ is bias. Here we have used batch version of gradient descent or steepest descent algorithm, in which we first start with some initial guess for the weight vector (which is often chosen at random) and then iteratively update the weight vector to minimize an error function equal to mean square difference between the desired and the actual output such that at step $n$

$$\Delta w^{(n)} = -\eta \nabla E\,|_{w^{(n)}} + \mu \Delta w^{(n-1)},$$

where $\eta$ is learning parameter and $\mu$ is momentum parameter. The ANN architecture used in this study consists of one input layer (with four to nine neurons or nodes), one hidden layer (with 16 neurons or nodes) and one output layer (with one neuron or nodes).

From the database composed of the simulated TBs for the TMI configuration and corresponding atmospheric profiles of the parameters of interest, ANN algorithm is used to derive the weights and the residual error of the algorithm. The ANN architecture used in this study consists of an input layer, a hidden layer, and an output layer. The nine inputs used in the ANN are radiative transfer simulated TBs corresponding to 10.7 GHz (V, H), 18.7 GHz (V, H), 21 GHz (V), 37 GHz (V, H) and 85 GHz (V, H) of TMI instrument onboard TRMM. The outputs are the ECMWF fields of TPW, CLW and SSW which were also used as inputs for the simulations. The training cycle involved forward feeding TB values in the training set from the input layer to the output layer to calculate the three mapping errors associated with TPW, CLW and WS separately and then backward propagating the mapping errors from the output layer to the input layer by adjusting the weights in the ANN. The root mean square error is calculated after all the input and output pairs in the training set are processed. The training is stopped in all the three cases when the rms error converged to a specified rms tolerance. The tolerance limit used for training is 0.0 and that is the tolerance limit for the simple error (desired-obtained) not for the RMSE. A total of 25,368 simulated TBs input profile database for the above-mentioned 9 channels of TMI with output data of TPW, CLW and WS were used separately. Out of this total database, 20,000 were used in training and the rest 5368 for testing the algorithm in all the three cases. All the three parameters achieved best performance of the ANN with different architectures respectively with variation in number of nodes in input and hidden layers (e.g. 4 to 9 nodes in the input

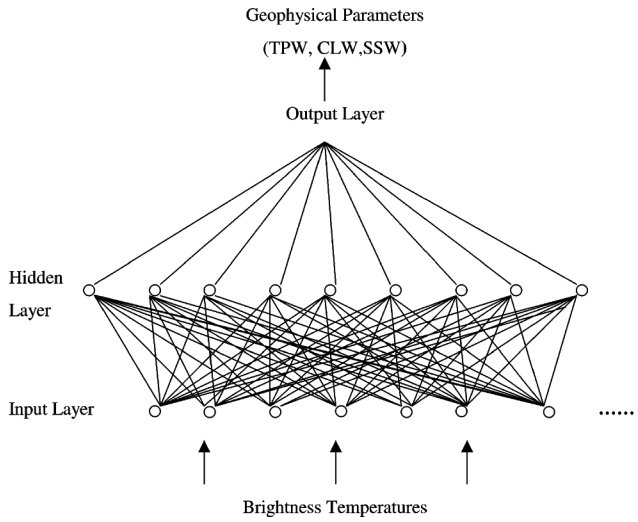


**Figure 1.** A neural network architecture connecting inputs (brightness temperatures) and output (TPW, CLW, SSW).

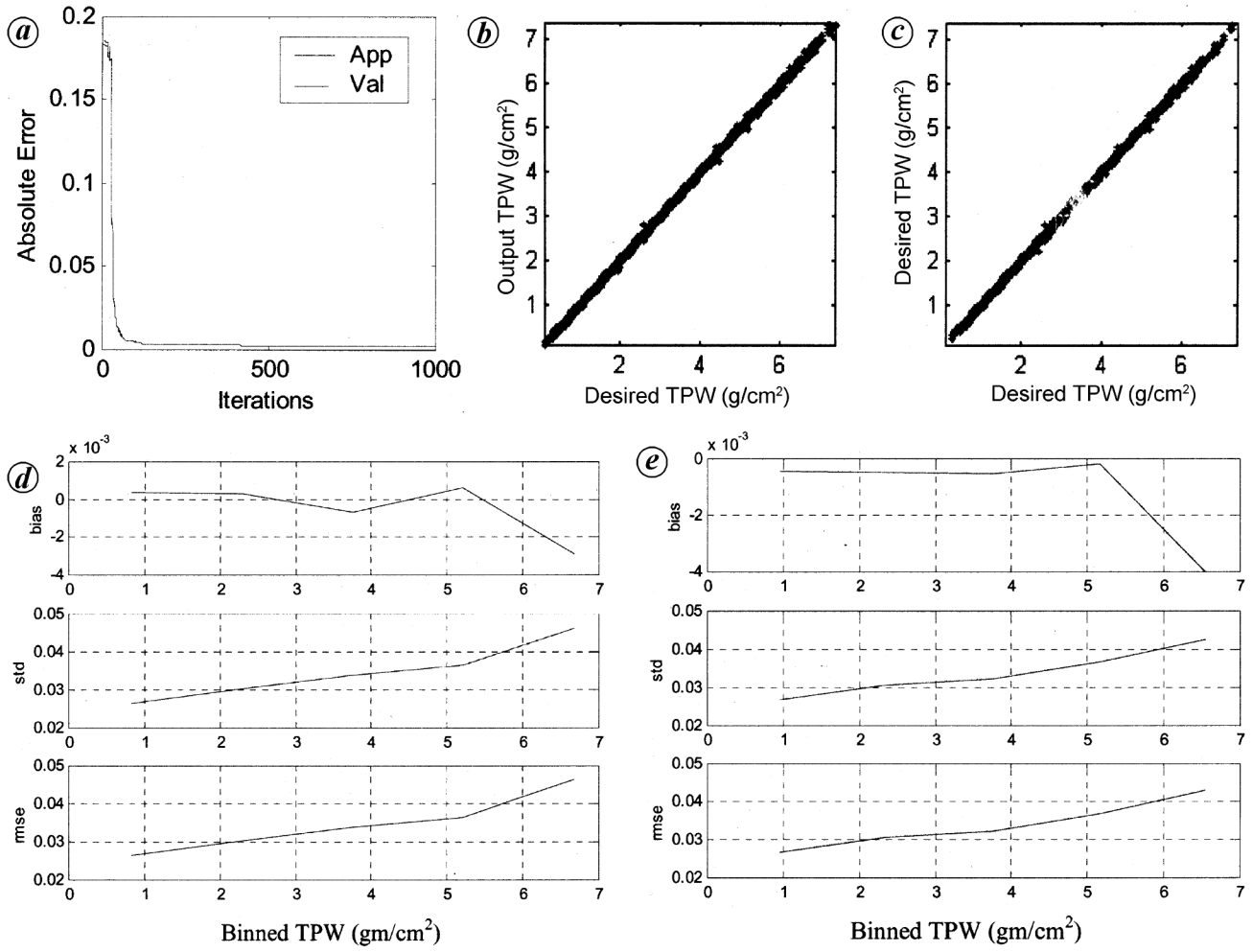


**Figure 2.** *a*, Distribution of global error. Desired vs ANN retrieved TPW for *b*, Training data set; *c*, Testing data set. Binned TPW (g/cm$^2$) *d*, Training data set; *e*, Testing data set.

layer and similarly different no. of nodes in the hidden layer) and number of iterations for the respective parameters. The inputs (TBs corresponding to the 10, 19, 21, 37 and 85 GHz channels) are processed with the number of nodes of hidden layer and then hidden layer nodes are processed with output node. The values of the learning rate parameter used for the ANN training were taken as 0.001 to 0.05 and the momentum parameter as 0.01 to 0.03 in the three cases. The analysis of the results is presented below for each parameter separately and briefly.

Figure 2 *a* shows the distribution of error with number of iterations during learning (continuous line) and testing phase (dashed line). It is evident that in case of water vapour the error drops very sharply within a few hundred iterations and later becomes almost constant, till more iterations are allowed to ensure that the ANN had learned the large values equally well as the small values. At this point the ANN is considered to be trained. The merger of continuous and dotted lines clearly shows that the data has been squashed well before separating into the training and testing sets and thus covering similar dynamic ranges in both sets and coincidentally the final ANN architecture leads to similar curves almost overlapping each other. The continuous black line has been marked as App to represent an application of ANN to the training data and blue line to represent the validation as Val for the testing data set. Figure 2 *b*, *c* shows the corresponding distributions of the desired and the ANN retrieved TPW for learning (20,000) and testing (5368) data sets respectively. The error statistics of these data distribution is shown in Table 1 for the training and testing data sets respectively.

There are significant correlations of 0.99 achieved in both cases of training and testing data sets. The average rms error and bias of 0.03321 and 0.0325 respectively are also very statistically significant. These are encouraging results and thus we also critically examine the running error estimates (i.e. the bias, standard deviation and rms error respectively) for each bin of TPW for both training and testing sets of data in Figure 2 *d*, *e*. In both cases, the rms

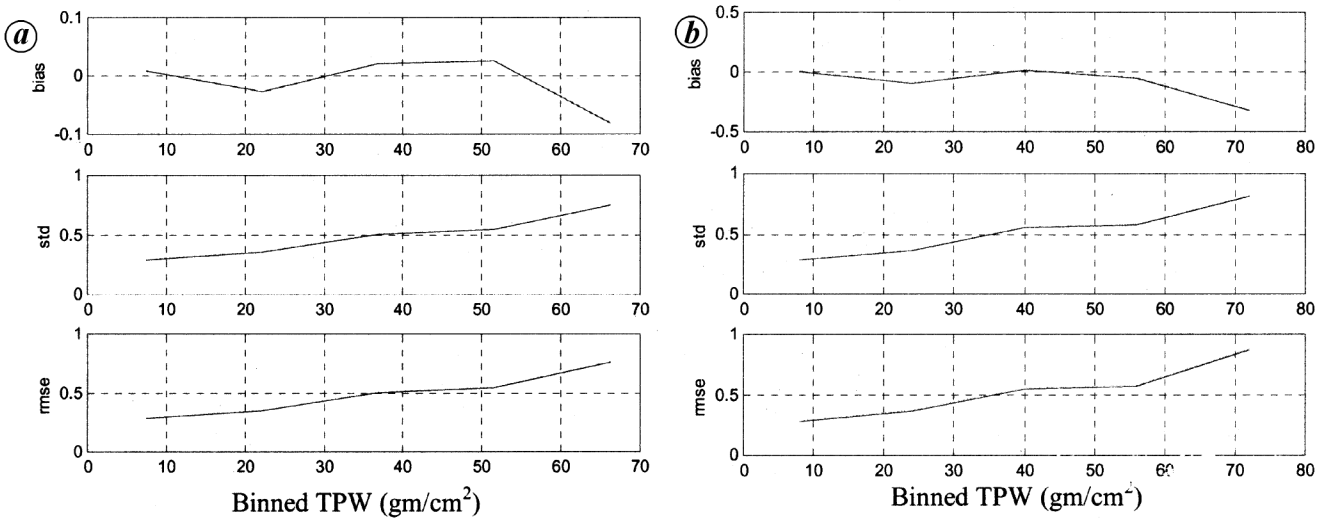


**Figure 3.** Binned CLW. *a*, Training data set; *b*, Training data set.

**Table 1.** Statistics of the input database

| | Training phase | Testing phase |
|---|---|---|
| No. of data points | 20000 | 5368 |
| Correlation coefficient | 0.990 | 0.990 |
| Bias | 0.0054 | –0.0056 |
| Standard deviation | 0.0322 | 0.0319 |
| RMS error | 0.0332 | 0.0325 |

error, standard deviation and bias are highest after 5.0 g/cm$^2$ of TPW. However these values of error estimates are very marginal and the average error estimates shown in Figure 2 *b*, *c* could be considered statistically representative for both training and testing cases.

A similar experiment has been performed for the CLW to evaluate the performance of ANN. The dynamic range of liquid water in ECMWF fields was found from 0 to 248.03 mg/cm$^2$. However, above 80 mg/cm$^2$, CLW is considered raining to heavy raining situations. Thus the results of radiative transfer simulations for the ECMWF profiles with CLW only up to 80 g/cm$^2$ are taken for consideration in ANN learning and testing procedures. This reduced the total number of data points by less than 10% only, as such cases that have been encountered during the simulations are very limited. However the data of input and output field vectors are partitioned in similar proportion as for TPW in order to retain the dynamic interdependency of the ocean and atmospheric variables represented in the database.

Similarly, the time evolution of error during the training and testing phases was of similar nature (not shown for brevity). A high correlation coefficient of 0.99 and rms error less than 0.9 mg/cm$^2$ in both cases was found encouraging for CLW which has nonlinear response with brightness temperatures due to the high degree of emission and Rayleigh scattering from the cloud drops. Due to this inherent nonlinearity of TBs and CLW relationship, we have experimented here with more number of hidden neurons keeping the other criteria of input and output channels common. The number of hidden neurons is proportional to the flexibility of ANN; the more the number of neurons used, the better is reproduction of the training data. Nevertheless too many neurons may result in larger errors for independent test set. Figure 3 *a*, *b* shows the root mean square error (rmse), standard deviation (sd) and bias with the binned CLW in both training and testing data cases respectively which are all mutually consistent and show that the bias and rms errors are higher with sd after 60 mg/cm$^2$ of CLW in both the cases. Still the percentage of this rms error is quite less and thus it indicates that better performance of ANN architecture is finally achieved.

The scanning radiometer TMI aboard TRMM, has made it possible to examine the benefits of 10 GHz channel to radiometric wind estimates. This channel provides a more transparent window to the ocean surface, and shows good sensitivity to the wind modulated ocean surface roughness. In addition, among all the TMI channels, it is this channel which has the maximum cloud penetration capability and thus provides ample opportunity for the retrieval of ocean surface parameters during the significant cloud cover conditions[22]. These advantages of the 10 GHz channels thus can also be used for the optimization and selection of suitable combination of other frequency channels in forthcoming satellite missions. Here we have attempted to explore the capability of ANN for the wind retrievals with the same database through radiative transfer simulations. The application of ANN to this database shows a correlation coefficient of 0.998 and 0.970 that is achieved in both training and testing cases with the learning rate and momentum parameter chosen within the range men-

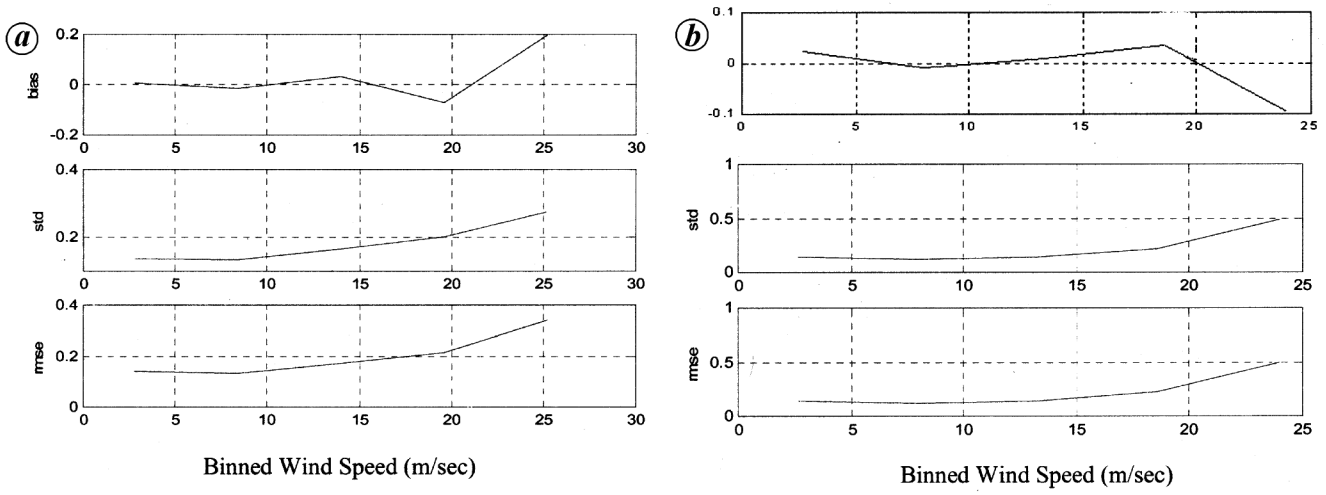


**Figure 4.** Binned wind speed (m/s). ***a***, Training data set; ***b***, Testing data set.

tioned above. For brevity only the figures for the error statistics and their running distributions with binned wind speed are shown in Figure 4 *a*, *b* respectively for training and testing cases.

The bias and root mean square error (rmse) are minimum below 0.25 m/s up to 20 m/s wind conditions which goes up by 0.5 m/s for winds at 20 to 25 m/s. This is because above 20 m/s, the weather conditions are not only rough over the oceans but also the associated surface convergence is associated with the atmospheric loading of CLW and rain and thus the error sources are increased. Here the TBs from the channel combinations of 37 GHz and below are opted as the input vectors (7 inputs of TBs) for the ANN training and testing along with the ECMWF surface winds (as output). It is evident from Figure 4 *a*, *b* that the performance of ANN is highly desirable for the retrieval of wind speed. Though the optimization of channel combination is further being performed with more sensitivity experiments, the results in all the three cases above are highly encouraging to look forward for the ANN approach to be adopted for the retrieval from forthcoming spaceborne microwave observations.

The potential of ANN for the development of retrieval algorithms for TPW, CLW and ocean surface winds from TRMM-TMI are studied. The present study has demonstrated the major aspects of retrieval of oceanic and atmospheric parameters followed from the sensitivity studies carried out through radiative transfer model simulations for rain-free atmospheric conditions over the oceans. Various architectures of the ANN have been experimented and the results are quite satisfactory in demonstrating the performance of ANN for the possible retrievals of all the three geophysical parameters from microwave radiometry with TRMM-TMI type of sensor. The study is aimed to ascertain the accurate retrievals of the geophysical parameters to be obtained from the MADRAS sensor of the Indo-French joint mission, MEGHA-TROPIQUES over the tropical regions which will be launched sometime in this decade. Timely, the recent Bay of Bengal Monsoon Experiment (BOBMEX)[22] during July–August 1999 and Arabian Sea Monsoon Experiment (ARMEX) during July–August 2002 and 2003, have made it possible to upgrade several instruments in ships (e.g. *Sagar Kanya* of Department of Ocean Development) for the availability of basic surface meteorological and oceanographic data under the Indian Climate Research Programme (ICRP). Ground-based upward looking radars are also being studied for the observation of the CLW and TPW measurements. Thus the validation of these retrievals could be planned for acquisition of ample database for the fine tuning of the algorithms well before the launch of the satellite.

1. Chou, S.-H., Shie, C.-L., Atlas, R. M. and Ardizzone, J., Air-sea fluxes retrieved from special sensor microwave imager data. *J. Geophys. Res.*, 1997, **102**, 12,705–12,726.
2. Ardizzone, J., Atlas, R., Jusem, J. C. and Hoffman, R. N., Application of SSM/I wind speed data to weather analysis and forecasting. 15th Conference on Weather Analysis and Forecasting, Am. Meteorol. Soc, Norfolk, 1996.
3. Deblonde, G. and Wagneur, N., Evaluation of global numerical weather prediction analyses and forecasts using DMSP special sensor microwave imager. *J. Geophys. Res.*, 1997, **102**, 1833–1850.
4. Beale, R. and Jackosn, T., *Neural Computing: An Introduction*, Adam Hilger, Bristol, 1990.
5. Hornik, K., Stinchombe, M. and White, H., Multilayer feedforward networks are universal approximators. *Neural Networks*, 1989, **2**, 359–366.
6. Goodberlet, M. A., Swift, C. T. and Wilkerson, J. C., Remote sensing of ocean surface winds with the special sensor microwave imager. *J. Geophys. Res.*, 1989. **94**, 14,547–14,555.
7. Gairola, R. M. and Pandey, P. C., *Proc. Indian Acad. Sci. (Earth Planet. Sci.)*, 1986, **95**, 265–273.
8. Alishouse, J. C., Snyder, S. A., Vongsathorn, J. and Ferraro, R. R., Determination of oceanic total precipitable water from the SSM/I. *IEEE Trans. Geosci. Remote Sens.*, 1990, **28**, 811–816.
9. Gairola, R. M., Gohil, B. S. and Pandey, P. C., *Remote Sens. Environ.*, 1985, **18**, 125–135.

10. Pandey, P. C., Gohil, B. S. and Hariharan, T. A., *IEEE Trans. Geosci. Remote Sens.*, 1984, **18**, 125–131.
11. Alishouse, J. C. *et al.*, Determination of cloud liquid water content using the SSM/I data. *IEEE Trans. Geosci. Remote Sens.*, 1990, **28**, 817–822.
12. Karstens, U., Simmer, C. and Ruprecht, E., Remote sensing of cloud liquid water. *Meteorol. Atmos. Phys.*, 1994, **54**, 157–171.
13. Gérard, E. and Eymard, L., Remote Sensing of integrated cloud liquid water: development of algorithms and quality control. *Radio Sci.*, 1998, **33**, 433–447.
14. Varma, A. K., Pokhrel, S., Gairola, R. M. and Agarwal, V. K., *IEEE Trans. Geosci. Remote Sens.*, 2003, **41**, 1–8.
15. Obligis, E., Eymard, L. and Gairola, R. M., 2nd ISRO-CNES Science Workshop on MEGHA-TROPIQUES, Paris, 2001.
16. Jung, T., Ruprecht, E. and Wagner, F., Determination of cloud liquid water path over the oceans from SSM/I data using neural networks. *J. Appl. Meteorol.*, 1998, **37**, 832–844.
17. Moreau, E., Mallet, C., Thiura, S., Mabboux, B. and Clapisz, C., Atmospheric liquid water retrieval using a gated expert neural network. *J. Atmos. Ocean. Technol.*, 2002, **19**, 457–467.
18. Prigent, C. and Abba, P., Sea surface equivalent brightness temperature at millimeter wavelength. *Ann. Geophys.*, 1990, **8**, 627–634.
19. Lippmann, R. P., An introduction to computing with neural nets. *IEEE ASSP Mag.*, 1987, **4**, 4–22.
20. Rumelhart, D. E., Hinton, G. E. and Williams, R. J., *Learning Representations by Back-propagating Errors*, MIT Press, Cambridge, Mass, 1986, pp. 318–362.
21. Wentz, F. J., A well-calibrated ocean algorithm for. SSM/I. *J. Geophys. Res.*, 1997, **102**, 8703–8718.
22. Bhat, G. S. *et al.*, BOBMEX – the Bay of Bengal monsoon experiment. *Bull. Am. Meteorol. Soc.*, 2001, **82**, 2217–2243.

ACKNOWLEDGEMENTS. We thank Director, Space Applications Centre for his interest and encouragement. Help from Dr E. Moreou, Dr Catherine Prigent and Dr Laurence Eymard of CNRS, France is acknowledged for providing the details of neural networks and the radiative transfer models respectively. We thank the referees for critically examining and making valuable suggestions to enhance the quality of the paper.

Received 17 September 2004; revised accepted 26 July 2006

# Natural radioactivity of ash and coal in major thermal power plants of West Bengal, India

**T. Mondal, D. Sengupta* and A. Mandal**

Department of Geology and Geophysics, Indian Institute of Technology, Kharagpur 721 302, India

**Natural radioactivity due to the presence of $^{238}$U, $^{232}$Th and $^{40}$K in ash and coal in major thermal power plants of West Bengal, namely Kolaghat, Durgapur and Bandel, has been measured by a NaI (Tl)-based gamma ray spectrometer. The average activity concentrations of the radioelements $^{238}$U, $^{232}$Th and $^{40}$K in the ashes of Kolaghat were found to be 111, 140 and 351 Bq/kg respectively, at Durgapur 97, 107 and 315 Bq/kg respectively, and at Bandel 106, 126 and 321 Bq/kg respectively. The absorbed gamma doses in air due to naturally occurring radionuclides in the ash from the power plants varied from 123 to 150 nGy h$^{-1}$, which are higher than three times the world average of about 43 nGy h$^{-1}$. The ash from power plants contains 2 to 3 times more natural radionuclides than that in feed coal. Ash samples have radium equivalent activity ($Ra_{eq}$) and external hazards index ($H_{ex}$) values closest to 370 Bq/kg and unity respectively, which have implications in terms of radiation hazard arising due to the use of these ash samples in building and construction.**

**Keywords:** Ash, coal, radioactivity, thermal power plants.

COAL is an important source of power generation in India. The country has at present 90,000 MW of electricity generation, of which coal combustion contributes to more than 70% of the power generation. Hydroelectricity contributes to about 25% and the remaining is from nuclear power plants[1]. Combustion of coal results in generation of huge amounts of ash, which is a major environmental problem. This problem is particularly important for Indian power stations because most of them use poor quality coal with 55–60% ash content. This results in an average production of 100 million tons of ash per annum[2]. In the combustion process, most of the mineral matter in coal is converted into ash. Solid wastes produced from the coal-fired thermal power plants are mainly of two types, i.e. fly ash and bottom ash. Bottom ash is the coarse-grained fraction that is collected from the bottom of the boiler and is disposed by the wet disposal method in a slurry form to nearby waste-disposal sites (ash ponds). Owing to its relatively small size and hence large surface area, ash has a greater tendency to absorb trace elements that are transferred from coal to waste products during combustion[3]. Most of the toxic elements (As, Cd, Cr, Ni, Co, Cu and Sb) become enriched in the soil and groundwater through leaching form the bottom ash, causing soil and water pollution.

Coal, like most materials found in nature, contains trace quantities of naturally occurring radionuclides, $^{238}$U, $^{232}$Th and $^{40}$K. Combustion of coal thus enhances natural radiation in the vicinity of the thermal power plants by release of these radionuclides and their daughters into the surrounding ecosystem. Unlike most of the nuclear and hydroelectric power stations, coal-fired power stations in India are generally located in areas which are thickly populated and, hence, the environmental impact experienced by the neighbouring population is significant. Apart from inhalation, an additional radiation hazard can be solid fallout resulting in elevated concentrations of natural radionuclides in the surface soils around the power

*For correspondence. (e-mail: dsgg@gg.iitkgp.ernet.in)